Construction of a genetic toggle switch in *Escherichia coli*

Timothy S. Gardner*†, Charles R. Cantor* & James J. Collins*†

** Department of Biomedical Engineering, † Center for BioDynamics and ‡ Center for Advanced Biotechnology, Boston University, 44 Cummington Street, Boston, Massachusetts 02215, USA*

It has been proposed[1] that gene-regulatory circuits with virtually any desired property can be constructed from networks of simple regulatory elements. These properties, which include multistability and oscillations, have been found in specialized gene circuits such as the bacteriophage λ switch[2] and the Cyanobacteria circadian oscillator[3]. However, these behaviours have not been demonstrated in networks of non-specialized regulatory components. Here we present the construction of a genetic toggle switch—a synthetic, bistable gene-regulatory network—in *Escherichia coli* and provide a simple theory that predicts the conditions necessary for bistability. The toggle is constructed from any two repressible promoters arranged in a mutually inhibitory network. It is flipped between stable states using transient chemical or thermal induction and exhibits a nearly ideal switching threshold. As a practical device, the toggle switch forms a synthetic, addressable cellular memory unit and has implications for biotechnology, biocomputing and gene therapy.

The design and construction of synthetic gene-regulatory networks would be greatly facilitated by a theory with predictive capability. Previous work using a reconstituted enzyme system[4] showed that nonlinear mathematics can predict qualitative behaviours of biochemical reaction networks, including multistability and hysteresis. However, a practical theory of gene-regulatory networks has lagged behind that of enzyme regulatory networks. A variety of physical and mathematical approaches, including logical (discrete)[5–10], piecewise linear[11], nonlinear[12–14], statistical–mechanical[15,16] and stochastic[17–19] formulations of the underlying biochemical dynamics, have been used in the past. Owing to the difficulty of testing their predictions, these theories have not, in general, been verified experimentally. Here we have integrated theory and experiment by constructing and testing a synthetic, bistable gene circuit based on the predictions of a simple mathematical model.

The toggle switch is composed of two repressors and two constitutive promoters (Fig. 1). Each promoter is inhibited by the repressor that is transcribed by the opposing promoter. We selected this design for the toggle switch because it requires the fewest genes and *cis*-regulatory elements to achieve robust bistable behaviour. By robust, we mean that the toggle exhibits bistability over a wide range of parameter values and that the two states are tolerant of the fluctuations inherent in gene expression (the toggle switch will not flip randomly between states). Although bistability is theoretically possible with a single, autocatalytic promoter, it would be less robust and more difficult to tune experimentally. In addition, the chosen toggle design does not require any specialized promoters, such as the P_R/P_{RM} promoter of bacteriophage λ. Bistability is possible with any set of promoters and repressors as long as they fulfil the minimum set of conditions described in Box 1 and Fig. 2.

The bistability of the toggle arises from the mutually inhibitory arrangement of the repressor genes. In the absence of inducers, two stable states are possible: one in which promoter 1 transcribes repressor 2, and one in which promoter 2 transcribes repressor 1. Switching is accomplished by transiently introducing an inducer of the currently active repressor. The inducer permits the opposing repressor to be maximally transcribed until it stably represses the originally active promoter.

All toggle switches are implemented on *E. coli* plasmids conferring ampicillin resistance and containing the pBR322 ColE1 replication origin. The toggle switch genes are arranged as a type IV plasmid, as shown in Fig. 3. Although all genes and promoters are

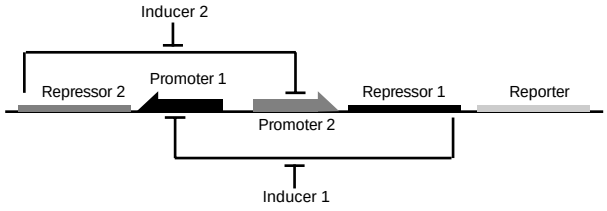

Figure 1 Toggle switch design. Repressor 1 inhibits transcription from Promoter 1 and is induced by Inducer 1. Repressor 2 inhibits transcription from Promoter 2 and is induced by Inducer 2.

Box 1

The toggle model

The behaviour of the toggle switch and the conditions for bistability can be understood using the following dimensionless model for the network:

$$\frac{du}{dt} = \frac{\alpha_1}{1+v^{\beta}} - u \quad (1a)$$

$$\frac{dv}{dt} = \frac{\alpha_2}{1+u^{\gamma}} - v \quad (1b)$$

where u is the concentration of repressor 1, v is the concentration of repressor 2, α_1 is the effective rate of synthesis of repressor 1, α_2 is the effective rate of synthesis of repressor 2, β is the cooperativity of repression of promoter 2 and γ is the cooperativity of repression of promoter 1. The above model is derived from a biochemical rate equation formulation of gene expression[24–27]. The final form of the toggle equations preserves the two most fundamental aspects of the network: cooperative repression of constitutively transcribed promoters (the first term in each equation), and degradation/dilution of the repressors (the second term in each equation).

The parameters α_1 and α_2 are lumped parameters that describe the net effect of RNA polymerase binding, open-complex formation, transcript elongation, transcript termination, repressor binding, ribosome binding and polypeptide elongation. The cooperativity described by β and γ can arise from the multimerization of the repressor proteins and the cooperative binding of repressor multimers to multiple operator sites in the promoter. An additional modification to equation (1) is needed to describe induction of the repressors (Fig. 5).

The geometric structure of equation (1), illustrated in Fig. 2a and b, reveals the origin of the bistability: the nullclines ($du/dt = 0$ and $dv/dt = 0$ in Fig. 2) intersect at three points, producing one unstable and two stable steady states. From Fig. 2a and b, three key features of the system become apparent. First, the nullclines intersect three times because of their sigmoidal shape, which arises for $\beta, \gamma > 1$. Thus, the bistability of the system depends on the cooperative repression of transcription. Second, the rates of synthesis of the two repressors must be balanced. If the rates are not balanced, the nullclines will intersect only once, producing a single stable steady state. This situation arises in plasmid pIKE105. Third, the structure of the toggle network creates two basins of attraction. Thus, a toggle with an initial condition anywhere above the separatrix will ultimately settle to state 1, whereas a toggle starting below the separatrix will settle to state 2.

The conditions for a bistable toggle network are illustrated in Fig. 2c and d. As the rates of repressor synthesis are increased, the size of the bistable region increases. Furthermore, the slopes of the bifurcation lines, for large α_1 and α_2, are determined by β and γ. Thus, to obtain bistability, at least one of the inhibitors must repress expression with cooperativity greater than one. Moreover, higher order cooperativity will increase the robustness of the system, allowing weaker promoters to achieve bistability and producing a broader bistable region.

contained on a single plasmid, they could, in principle, be divided into two separate plasmids without altering the functionality of the toggle. Two classes of toggle switch plasmids were constructed—the pTAK class and the pIKE class. Both classes use the Lac repressor (*lacI*) in conjunction with the Ptrc-2 promoter for one promoter–repressor pair. For the second promoter–repressor pair (P1, R1 in Fig. 3), pTAK plasmids use the P_Ls1con promoter in conjunction with a temperature-sensitive λ repressor (*cIts*), whereas pIKE plasmids use the $P_L$tetO-1 promoter in conjunction with the Tet repressor (*tetR*). pTAK plasmids are switched between states by a pulse of isopropyl-β-D-thiogalactopyranoside (IPTG) or a thermal pulse. pIKE plasmids are switched between states by a pulse of IPTG or a pulse of anhydrotetracycline (aTc).

The promoters used in the toggle are $P_L$tetO-1 (ref. 20) (TetR repressed), Ptrc-2 (LacI repressed) and P_Ls1con (CI repressed). The ranked order of the transcriptional efficiencies of the promoters is P_Ls1con > Ptrc-2 > $P_L$tetO-1. In all variants of the toggle switch, the sequence of the three promoters is unchanged. The rates of synthesis of the repressors (α_1 and α_2 in the model) or the reporter genes are modified by exchanging the downstream ribosome binding sites (RBS). The promoter and RBS sequences and their relative strengths are described in the Supplementary Information.

In all toggle plasmids, the *gfpmut3* gene[21] is arranged as the second cistron downstream of the Ptrc-2 promoter. Thus, transcription from Ptrc-2, and hence, repression of P1, results in the expression of green fluorescent protein (GFP)mut3. For clarity, this state is termed the 'high' state. The opposing state, in which P1 is transcribed and Ptrc-2 is repressed, is termed the 'low' state. Unless otherwise indicated, *gfpmut3* is the reporter used in all plasmids.

To investigate the conditions required for bistability, six variants of the toggle switch (four pTAK plasmids and two pIKE plasmids) were constructed by inserting RBS sequences of differing strengths into the RBS1 site. All four pTAK plasmids exhibited bistability, whereas only one pIKE plasmid (pIKE107) exhibited bistability. The demonstration of bistability is illustrated in Fig. 4. In this experiment, the toggle and control plasmids were grown in *E. coli* strain JM2.300 for 23.5 h. At 6, 11 and 18 h, samples were washed and diluted into fresh medium with or without inducers, as appropriate. Cells were initially grown for 6 hours with 2 mM IPTG, inducing GFPmut3 expression in all toggles and the IPTG-inducible pTAK102 control plasmid. Cells were grown for an additional 5 h with no IPTG. The five bistable toggle plasmids, which had been switched to the high state, continued to express GFPmut3 in the absence of inducer, whereas the pTAK102 control plasmid and the monostable pIKE105 toggle plasmid returned to the low state. Cells were then grown at 42 °C (pTAK plasmids only) or grown in the presence of 500 ng ml^{-1} aTc (pIKE plasmids only). After 7 h of growth, GFPmut3 expression in all toggles was shut off, whereas GFPmut3 expression in the thermally-inducible pTAK106 control and the aTc-inducible pIKE108 control was activated. Cells were returned to standard temperature (see Methods) with no inducers. After an additional 5.5 h, the five bistable toggle plasmids remained in the low state, whereas the pTAK106 and pIKE108 controls returned, as expected, to their non-induced condition.

Figure 4c shows the long-term stability of the two states of the pTAK117 toggle plasmid. In this experiment, a single culture of pTAK117 cells (initially in the low state) was divided into two cultures. The first group was grown in medium with no inducers, while the second group was grown in medium with 2 mM IPTG. After 6 h, cells were washed and diluted into fresh medium with no inducer. Both groups of cells were grown for an additional 22 h, being sampled and diluted into fresh medium every 6–8.5 h. The two groups of pTAK117 cells remained in their initial high or low states for the entire 22 h.

Although all of the toggle plasmids contain the same configuration of elements, one plasmid, pIKE105, does not exhibit bistability. This result is probably due to the reduced efficiency of the Tet repressor relative to the λ repressor. To maintain bistability, the reduced efficiency requires a corresponding decrease in the strength of the $P_L$tetO-1 promoter relative to the P_Ls1con promoter (see Box 1). The $P_L$tetO-1 promoter in the pIKE105 plasmid is not sufficiently reduced in strength to achieve bistability. However, the strength reduction provided by the $P_L$tetO-1 promoter in the pIKE107 plasmid is sufficient.

A qualitative prediction of the toggle model is that a genetic toggle will have nearly ideal switching thresholds. Induction by IPTG, aTc or heat alters the dynamic balance between the competing promoters such that the toggle is pushed into a region of monostability. The transition from bistability to monostability occurs in a sharp, discontinuous fashion owing to the existence of a bifurcation. This bifurcation occurs when one of the stable steady states is annihilated by the unstable steady state.

The ideal threshold, or bifurcation, in the pTAK117 toggle switch is illustrated both theoretically and experimentally in Fig. 5. In this experiment, pTAK117 (initially in the low state) and pTAK102 (as a control) were grown in 13 different concentrations of IPTG for 17 h

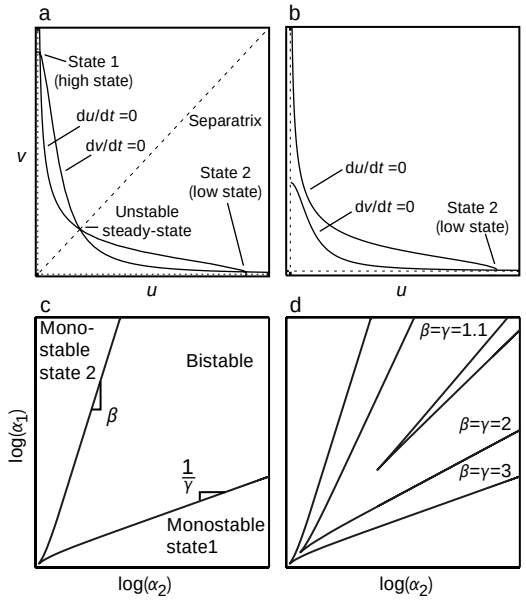

Figure 2 Geometric structure of the toggle equations. **a**, A bistable toggle network with balanced promoter strengths. **b**, A monostable toggle network with imbalanced promoter strengths. **c**, The bistable region. The lines mark the transition (bifurcation) between bistability and monostability. The slopes of the bifurcation lines are determined by the exponents β and γ for large α_1 and α_2. **d**, Reducing the cooperativity of repression (β and γ) reduces the size of the bistable region. Bifurcation lines are illustrated for three different values of β and γ. The bistable region lies inside of each pair of curves.

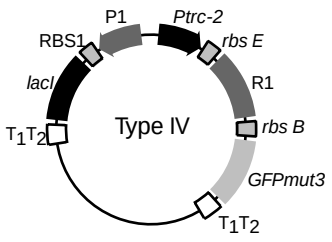

Figure 3 The toggle switch plasmid. Promoters are marked by solid rectangles with arrowheads. Genes are denoted with solid rectangles. Ribosome binding sites and terminators (T_1T_2) are denoted by outlined boxes. Different P1 promoters, RBS1 ribosome binding sites, and/or R1 repressors, are used for the various toggle switches. Plasmid types I–III, used in the construction and testing of the toggle components, are described in the Supplementary Information.

to steady state, being diluted twice (at 6 and 12.5 h) into fresh medium with the same IPTG concentration. Induction of the pTAK102 control has the familiar sigmoidal shape. In contrast, the pTAK117 toggle follows the induction curve of pTAK102 up to an IPTG concentration of 40 μM, at which point it crosses the bifurcation and exhibits a quasi-discontinuous jump to the high expression state. Owing to the natural fluctuations in gene expression, the bifurcation is not a perfect discontinuity as predicted by the deterministic toggle equations. The stochastic nature of gene expression causes variability in the location of the switching threshold and thus blurs the bifurcation point. Near the bifurcation, this blurriness is realized as a bimodal distribution of cells (Fig. 5c).

The switching time of the pTAK117 plasmid from the low to the high state and from the high to the low state is shown in Fig. 6. In this experiment, pTAK117 cells in the low state were diluted in fresh medium and induced with 2 mM IPTG. Separate cultures were grown for 35 min to 6 h before being washed and diluted in fresh medium with no inducer. Growth was continued until 10.25 h after the start of the experiment and cells were assayed in the flow cytometer. Conversely, pTAK117 cells in the high state were diluted in fresh medium with no inducer. Separate cultures were grown at 41 ± 1 °C for 35 min to 6 h before being diluted in fresh medium with no inducer. Growth was continued at standard temperature until 10.25 h after the start of the experiment and cells were assayed in the flow cytometer.

As shown by the appearance of a bimodal distribution at 4 h (Fig. 6), the pTAK117 plasmid begins switching to the high state after 3–4 h of IPTG induction. By 5 h the switching is nearly complete, and by 6 h it is complete. On the other hand, switching from the high state to the low state is completed in 35 min or less. The primary determinant of switching time is the rate of elimination of the repressor proteins. Switching from low to high requires the gradual dilution, by cell growth, of the IPTG-bound Lac repressor. On the other hand, switching from high to low is effected by immediate thermal destabilization of the temperature-sensitive λ repressor. Thus, switching to the low state is substantially faster than switching to the high state. Furthermore, the configuration of the pTAK117 plasmid—the rate of Lac repressor synthesis is more than an order of magnitude higher than the rate of λ repressor synthesis—suggests that the low state is more stable than the high state.

Our approach to the construction of a genetic toggle switch represents a significant departure from traditional genetic engineering in that we rely primarily on the manipulation of network

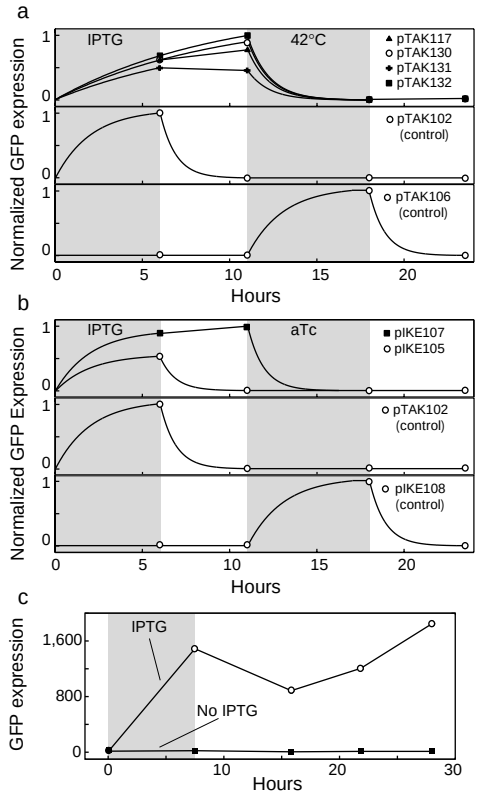

Figure 4 Demonstration of bistability. The grey shading indicates periods of chemical or thermal induction. The lines in **a** and **b**, which are approximations of the switching dynamics, are included for clarity. **a**, pTAK toggle plasmids and controls. **b**, pIKE toggle plasmids and controls. **c**, Demonstration of the long-term stability of the separate expression states in pTAK117.

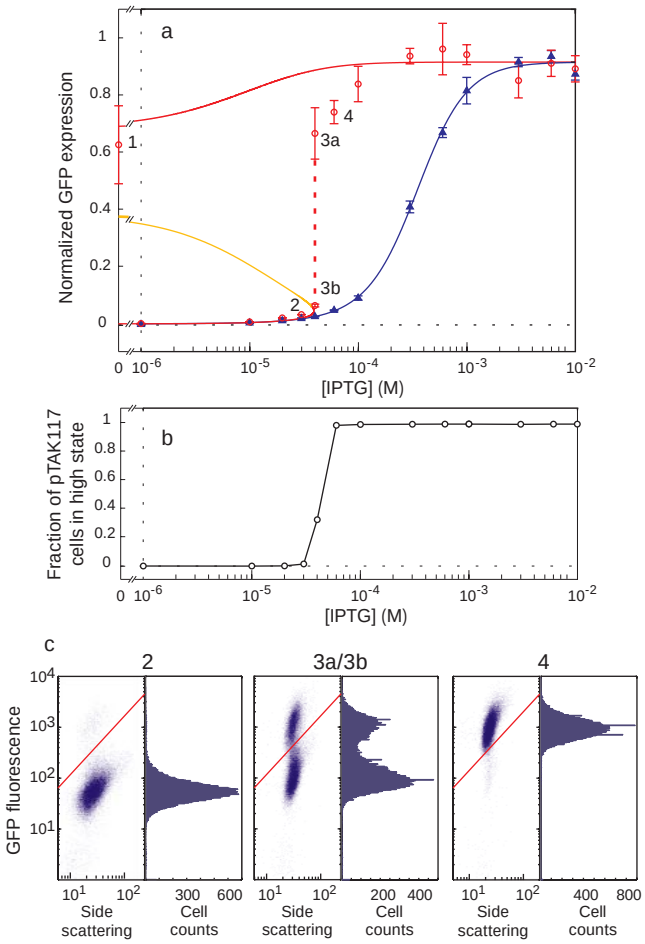

Figure 5 Toggle switch induction threshold. **a**, Steady-state gene expression after 17-h induction. The pTAK117 toggle plasmid (red circles) exhibits a quasi-discontinuous jump to the high state whereas the pTAK102 control plasmid (blue triangles) exhibits a sigmoidal induction curve. Point 1 is taken from separate experiments measuring the high state of pTAK117 with no inducer. Points 3a and 3b are the high and low modes of a bimodally distributed cell population. The bimodality occurs due to natural fluctuations in gene expression and the close proximity of the toggle switch to its bifurcation point. Theoretical curves are calculated from equation (1) with the term $u/(1 + [\mathrm{IPTG}]/K)^{\eta}$, where K is the dissociation constant of IPTG from LacR and η is the cooperativity of IPTG binding, replacing u in the denominator of equation (1b). The red curves show the stable steady states and the orange curve shows the unstable steady state of the toggle. The blue curve shows the steady state of the IPTG-inducible control plasmid. Model parameters for the theoretical curves are $\alpha_1 = 156.25$, $\alpha_2 = 15.6$, $\beta = 2.5$, $\gamma = 1$, $\eta = 2.0015$, $K = 2.9618 \times 10^{-5}$. **b**, Fraction of toggle cells in the high state at various concentrations of IPTG. The sudden switching to the high state is more clearly visible. High and low cell populations were divided as described for **c** below. **c**, Scatter plots (left plots) and histograms (right plots) illustrating the condition of the toggle cells at points 2, 3 and 4 (of **a**) near the bifurcation point. High-state and low-state cell populations are divided by the red line in the scatter plots. The two states of the toggle are clearly evident in the bimodally distributed cells (point 3).

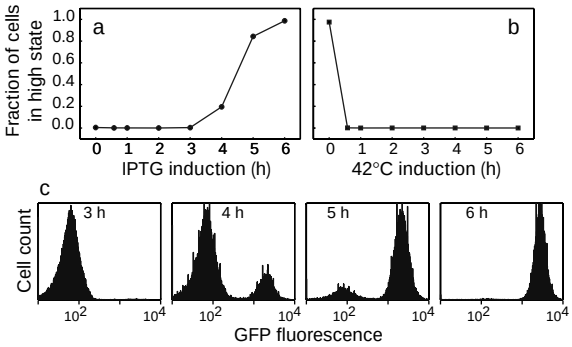

Figure 6 pTAK117 switching time. **a**, **b**, The fraction of cells in the high state is plotted as a function of the induction time. Cells were divided between high and low states as in Fig. 5c. **c**, Switching of pTAK117 cells from the low to the high state by IPTG induction. The cell population is illustrated at four time points. Cells begin switching between 3 and 4 h as shown by the appearance of a bimodal distribution. The switching is complete by 6 h.

architecture, rather than the engineering of proteins and other regulatory elements, to obtain desired behaviours. In addition, the reasonable agreement between the toggle theory and experiment indicates that the theoretical design of complex and practical gene networks is a realistic and achievable goal. Moreover, the genetic toggle switch exemplifies a forward engineering approach to the study of gene regulation in which synthetic gene circuits serve as highly simplified, highly controlled models of natural gene networks. As a practical device, the toggle switch, which requires only transient rather than sustained induction, may find applications in gene therapy and biotechnology. Finally, as a cellular memory unit, the toggle forms the basis for 'genetic applets'—self-contained, programmable, synthetic gene circuits for the control of cell function. □

Methods

Numerics

All theoretical curves were calculated numerically from equation (1) (Box 1) using Matlab (Mathworks), XPP-AUTO, software for simulation and analysis of differential equations (G. B. Ermentrout, University of Pittsburgh, available at http://www.pitt.edu/~phase/), or AUTO, a bifurcation package included in the XPP-AUTO software (E. Doedel, McGill University).

Plasmid construction

Plasmids were constructed using basic molecular cloning techniques as described in standard cloning manuals[22,23]. Restriction enzymes were from New England Biolabs and Promega; Pfu*Turbo* polymerase was from Stratagene; all other enzymes were from New England Biolabs; all synthetic oligonucleotides were from Operon Technologies. All genes, promoters and transcription terminators were obtained by PCR amplification using Pfu*Turbo* proofreading polymerase and synthetic primers with overhanging ends containing the appropriate restriction sites. Ribosome binding sites were included in the overhanging ends of the primers. Site mutations were performed using either Stratagene QuickChange or ExSite.

Genes, promoters and transcription terminators were obtained as follows: Ptrc-2 from pTrc99a (AP Biotech); P_L from pXC46 (ATCC); $p_L$tetO-1 by total synthesis according to the published sequence[20]; *lacI* from pTrc99a; *cIts* from pGW7 (ATCC); *tetR* from pcDNA6/TR (Invitrogen); *gfpuv* from pGFPuv (Clontech); *gfpmut3* from pJBA111 (gift of J. B. Andersen, Technical University of Denmark); and rrnT1T2 terminators from pTrc99a. All plasmids contained the ampicillin resistance region and ColE1 and origin of replication from the pTrc99a plasmid. All cloning was performed by TSS transformation[22] into *E. coli* strain JM2.300 (CGSC), JC158 (CGSC) or TAP106 (ATCC).

DNA sequencing was performed using a Perkin-Elmer ABI Prism 377 sequencer.

Strains, growth conditions and chemicals

The host cell for all promoter assays and toggle switch experiments was *E. coli* strain JM2.300 (λ–, *lacI22 rpsL135* (StrR), *thi-1*) (CGSC strain 5002). JM2.300, which contains few mutations, is a fast-growing strain that can tolerate enormous overexpression of plasmid-bound genes. Because JM2.300 contains no λ repressor and carries a nonfunctional Lac repressor (*lacI22*), it is an ideal host for the toggle switch.

All cells were grown in LB medium (Difco) with 100 μg ml^{-1} ampicillin plus inducers as indicated in the text. All Type I and pIKE series plasmids were grown at 37 ± 1 °C, unless otherwise indicated. All pTAK series plasmids were grown at 32 ± 1 °C except during thermal induction. Thermal induction was carried out at 42 ± 1 °C, unless otherwise indicated. For all expression tests, cells were maintained in logarithmic growth phase by periodic 500–1,000-fold dilution into fresh medium.

Ampicillin and IPTG were from Sigma. Anhydrotetracycline was from ACROS Organics. All other chemicals were from Fisher.

Assay of gene expression

All expression data were collected using a Becton–Dickinson FACSCalibur flow cytometer with a 488-nm argon excitation laser and a 515–545-nm emission filter. Before assay, cells were pelleted and resuspended in 0.22 μm filtered PBS (58 mM Na_2HPO_4, 17 mM NaH_2PO_4, 68 mM NaCl, pH = 7.4). Cells were assayed at low flow rate and fluorescence was calibrated using InSpeck green fluorescent beads (Molecular Probes). All measurements of gene expression were obtained from three independent cultures maintained simultaneously under identical conditions. For each culture, 40,000 events were collected. All flow data were converted to ASCII format using MFI (E. Martz, University of Masachusetts, Amherst, available at http://marlin.bio.umass.edu/mcbfacs/flowcat.html#mfi) and analysed with Matlab.

Received 15 September; accepted 23 November 1999.

1. Modod, J. & Jacob, F. General conclusions: teleonomic mechanisms in cellular metabolism, growth and differentiation. *Cold Spring Harb. Symp. Quant. Biol.* **26,** 389–401 (1961).
2. Ptashne, M. *A Genetic Switch: Phage λ and Higher Organisms* (Cell, Cambridge, Massachusetts, 1992).
3. Ishiura, M. *et al.* Expression of a gene cluster *kaiABC* as a circadian feedback process in cyanobacteria. *Science* **281,** 1519–1523 (1998).
4. Schellenberger, W., Eschrich, K. & Hofmann, E. Self-organization of a glycolytic reconstituted enzyme system: alternate stable stationary states, hysteretic transitions and stabilization of the energy charge. *Adv. Enzyme Regul.* **19,** 257–284 (1980).
5. Glass, L. & Kauffman, S. A. The logical analysis of continuous, non-linear biochemical control networks. *J. Theor. Biol.* **39,** 103–129 (1973).
6. Glass, L. Classification of biological networks by their qualitative dynamics. *J. Theor. Biol.* **54,** 85–107 (1975).
7. Glass, L. Combinatorial and topological methods in nonlinear chemical kinetics. *J. Chem. Phys.* **63,** 1325–1335 (1975).
8. Kauffman, S. The large scale structure and dynamics of gene control circuits: an ensemble approach. *J. Theor. Biol.* **44,** 167–190 (1974).
9. Thomas, R. Logical analysis of systems comprising feedback loops. *J. Theor. Biol.* **73,** 631–656 (1978).
10. Thomas, R. Regulatory networks seen as asynchronous automata: a logical description. *J. Theor. Biol.* **153,** 1–23 (1991).
11. Tchuraev, R. N. A new method for the analysis of the dynamics of the molecular genetic control systems. I. Description of the method of generalized threshold models. *J. Theor. Biol.* **151,** 71–87 (1991).
12. Arkin, A. & Ross, J. Computational functions in biochemical reaction networks. *Biophys. J.* **67,** 560–578 (1994).
13. Bhalla, U. S. & Iyengar, R. Emergent properties of networks of biological signaling pathways. *Science* **283,** 381–387 (1999).
14. Yagilo, G. & Yagil, E. On the relation between effector concentration and the rate of induced enzyme synthesis. *Biophys. J.* **11,** 11–27 (1971).
15. Shea, M. A. & Ackers, G. K. The O_R control system of bacteriophage Lambda: a physical-chemical model for gene regulation. *J. Mol. Biol.* **181,** 211–230 (1985).
16. Smith, T. F., Sadler, J. R. & Goad, W. Statistical–mechanical modeling of a regulatory protein: the Lactose repressor. *Math. Biosci.* **36,** 61–86 (1977).
17. Arkin, A., Ross, J. & McAdams, H. H. Stochastic kinetic analysis of developmental pathway bifurcation in phage λ-infected *Escherichia coli* cells. *Genetics* **149,** 1633–1648 (1998).
18. McAdams, H. H. & Arkin, A. Stochastic mechanisms in gene expression. *Proc. Natl Acad. Sci. USA* **94,** 814–819 (1997).
19. McAdams, H. H. & Arkin, A. Stimulation of prokaryotic genetic circuits. *Annu. Rev. Biophys. Biomol. Struct.* **27,** 199–224 (1998).
20. Lutz, R. & Bujard, H. Independent and tight regulation of transcriptional units in *Escherichia coli* via the LacR/O, the TetR/O and AraC/I_1-I_2 regulatory elements. *Nucleic Acids Res.* **25,** 1203–1210 (1997).
21. Cormack, B. P., Valdivia, R. H. & Falkow, S. FACS-optimized mutants of the green fluorescent protein (GFP). *Gene* **173,** 33–38 (1996).
22. Ausubel, F. M. *et al. Current Protocols in Molecular Biology* (Wiley, New York, 1987).
23. Sambrook, J., Fritsch, E. F. & Maniatis, T. *Molecular Cloning: A Laboratory Manual* (Cold Spring Harbor Laboratory Press, Plainview, New York, 1989).
24. Edelstein-Keshet, L. *Mathematical Models in Biology* (McGraw-Hill, New York, 1988).
25. Kaplan, D. & Glass, L. *Understanding Nonlinear Dynamics* (Springer, New York, 1995).
26. Yagil, E. & Yagil, G. On the relation between effector concentration and the rate of induced enzyme synthesis. *Biophys. J.* **11,** 11–27 (1971).
27. Rubinow, S. I. *Introduction to Mathematical Biology* (Wiley, New York, 1975).

Supplementary information is available at *Nature*'s World-Wide Web site (http://www.nature.com) or as paper copy from the London editorial office of *Nature*.

Acknowledgements

We thank M. Bitensky and T. Yoshida for providing access to their flow cytometer; Y. Yu for his suggestions on plasmid construction; C. Sabanayagam for his technical advice; and C. Chow for his mathematical advice. This work was supported by the Office of Naval Research and the College of Engineering at Boston University.

Correspondence and requests for materials should be addressed to J.J.C. (e-mail: jcollins@bu.edu). Plasmid sequences are available at http://cbd.bu.edu/abl/toggle.